

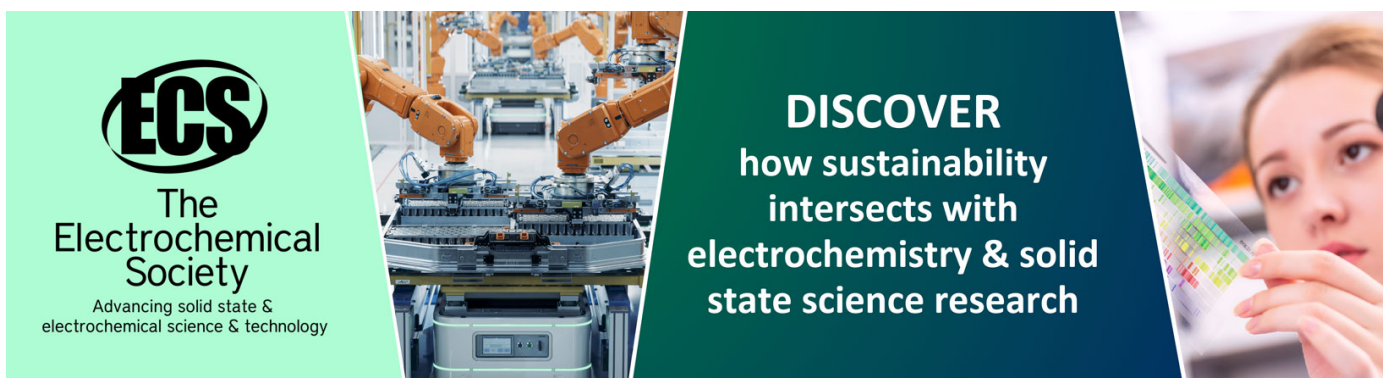
Theoretical and experimental study on ozone generation characteristics of an oxygen-fed ozone generator in silent discharge

To cite this article: J Kitayama and M Kuzumoto 1997 *J. Phys. D: Appl. Phys.* **30** 2453

View the [article online](#) for updates and enhancements.

You may also like

- [Development of ozone sterilization system based microcontroller for *E. Coli* bacteria sterilization](#)
Arfan Eko Fahrudin, Endarko, Amar Vijai Nasrulloh et al.
- [Power analysis of ozone generator for high capacity production](#)
E Yulianto, M Restiwijaya, E Sasmita et al.
- [Ozone production in parallel multichannel dielectric barrier discharge from oxygen and air: the influence of gas pressure](#)
Dingkun Yuan, Zhihua Wang, Can Ding et al.



ECS
The
Electrochemical
Society
Advancing solid state &
electrochemical science & technology

DISCOVER
how sustainability
intersects with
electrochemistry & solid
state science research

Theoretical and experimental study on ozone generation characteristics of an oxygen-fed ozone generator in silent discharge

J Kitayama^{†§} and M Kuzumoto^{†‡||}

[†] Manufacturing Engineering Centre, Mitsubishi Electric Corporation, 8-1-1 Tsukaguchihonmachi Amagasaki-city, Hyogo, Japan 661

[‡] Advanced Technology R&D Centre, Mitsubishi Electric Corporation, 8-1-1 Tsukaguchihonmachi Amagasaki-city, Hyogo, Japan 661

Received 21 January 1997, in final form 12 May 1997

Abstract. Experimental and theoretical investigations have been carried out on the ozone generation characteristics of oxygen-fed ozone generators with various discharge gap lengths. In this paper, a new theoretical model considering the dependence of ozone dissociation rate by electron impact on the electric field strength is suggested. Assuming a stationary and uniform discharge in time and space, ozone concentrations obtained experimentally under various discharge power densities and gas pressures are well explained by this model. It is concluded that the operation under a high electric field has a potential advantage in producing high-concentration ozone efficiently because of the reduction in the population density of low-energy electrons which decompose generated ozone.

1. Introduction

Ozone is one of the strongest oxidizing and bleaching agents without residues that could be harmful to the environment. For this reason, ozone has been used for a variety of applications such as bleaching, deodorization, and disinfection of water and atmospheric air. Recently, in the field of water purification, the use of ozonization is regarded as important in eliminating the precursor of trihalogenated methanes which are generated in chlorination process and are carcinogenic organic chlorides.

Ozone is almost exclusively produced by silent discharge (dielectric barrier discharge), the configuration first proposed by Siemens in 1857 [1]. In an ozone generator, the generation and decomposition of ozone occur concomitantly in the discharge space. Therefore, it is necessary for efficient production of high-concentration ozone to suppress ozone decomposition by electron impact. The mechanism of ozone generation in the silent discharge of an oxygen-fed ozone generator has been studied by several investigators [2, 3]. They assumed that the coefficient of ozone decomposition by electron impact is constant for every electric field strength they investigated. So, the experimental results by varying basic parameters such like discharge gap length and gas pressure could not be explained well.

[§] E-mail address: kitayama@ama.mdl.melco.co.jp

^{||} E-mail address: kuzumoto@ene.crl.melco.co.jp

In this paper, we report a new ozone generation model considering the dissociation rate of ozone by electron impact as a function of electric field strength in the discharge space. On the basis of reported dissociation cross sections of ozone, we obtained the dissociation rate of ozone as a function of electric field strength by Boltzmann equation analysis. By using this rate coefficient, experimental results are shown to be analysed accurately over a broad discharge gap length range of 50 μm –1.0 mm.

2. Experimental investigation

Basic parameters related to the excitation of particles by discharge were obtained experimentally. In the experiments we used a new plate type ozone generator [4] and a conventional tube type ozone generator [5]. In this section, we estimate some physical quantities in the discharge space from experimental results.

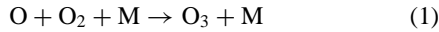
2.1. Reduced electric field strength

Discharge voltages V^* at gas temperature 288 K were evaluated by V - Q Lissajous figures and are plotted against the pd product (the product of gas pressure and discharge gap length), as shown in figure 1. In this figure, \circ indicates the experimental results of the tube type ozone generator (discharge gap length d : 0.6–1.2 mm, dielectric

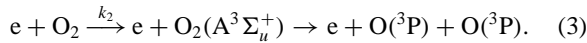
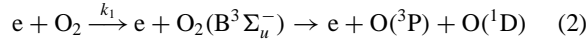
material: glass), while □ indicates the results of the new plate type ozone generator (discharge gap length d : 0.05–0.2 mm, dielectric material: ceramics). Discharge voltages V^* have no dependence on electrode materials. The average electric field strength in the discharge space is obtained by dividing discharge voltage by the pd product, illustrated by the three solid lines in figure 1. It is around 100 Td (1 Td = 10^{-17} V cm $^{-2}$) under the operating conditions of the conventional tube type ozone generator ($pd = 100$ Torr cm). On the other hand, by using the new plate type ozone generator, it is possible to form a discharge space with high electric field strength (around 300 Td), operating over a lower pd product region than the conventional operating conditions. We use the estimated value of E/N from this experimental result in the analysis of ozone generation discussed in section 4.

2.2. Energy consumption by electrons

Ozone is generated through the three-body collision reaction shown in reaction (1).



where M is the third collision partner, for example, O, O₂ and O₃ for an oxygen-fed ozone generator. Oxygen atoms are generated by collisions between oxygen molecules and electrons in the discharge space. This process is divided into the following reactions: the Schumann–Runge system (B³Σ_u⁻, threshold: 8.4 eV) and the Hertzberg system (A³Σ_u⁺, threshold: 6 eV).



We let the dissociation rate coefficients for the above two reactions be k_1 and k_2 , respectively. Since O(D) generated by reaction (2) is immediately transformed into O(P) through collisions with oxygen molecules, two oxygen atoms are generated by either reaction (2) or (3) per collision. So, the number of oxygen atoms O(P) produced by one electron per cm of path is

$$n_1 = 2(k_1 + k_2) \frac{N}{v_{de}} \quad (4)$$

where N is the particle density of oxygen molecules (particles cm⁻³) and v_{de} is the drift velocity of electrons (cm s⁻¹).

The energy which an electron obtains in the electric field per cm of path is given by

$$\Delta E_e = eE \quad (5)$$

where e is the charge of an electron, and E is the electric field strength. Assuming the portion of energy carried by electrons to be κ , the total energy gained by a charged particle in the electric field per cm of path is given by

$$\Delta E_t = \frac{\Delta E_e}{\kappa} \quad (6)$$

Former investigators estimated κ to be 0.5 because the silent discharge is considered to be developed to the stage of the streamer discharge, where electrons and positive ions are produced evenly along the discharge columns [2]. From equations (4)–(6), the energy required to obtain one oxygen atom is given by

$$\frac{n_1}{\Delta E_t} = \kappa \frac{2(k_1 + k_2)}{ev_{de}(E/N)} \quad (7)$$

The dissociation rate coefficients k_1 , k_2 and drift velocity of electrons are obtained by solving the Boltzmann equation for each E/N . The relationship between the efficiency and E/N for $\kappa = 1$ (namely, in the case that input energy is consumed only by electrons) in equation (7) is depicted by the dotted curve in figure 2. This curve also shows the maximum obtainable efficiency for ozone formation, provided that every oxygen atom combines with one oxygen molecule to form one ozone molecule.

The experimental results of ozone yield obtained at extremely low ozone concentrations are also plotted in figure 2. The data for the discharge gap length from 0.05 to 0.2 mm are obtained by a ceramic plate electrode (the plate type ozone generator), while the data for the discharge gap length from 0.5 to 1.0 mm are obtained by a glass tube electrode (the tube type ozone generator). Because every oxygen atom generated by dissociation is thought to be transformed into ozone at extremely low ozone concentration, we can define this ozone yield as the maximum one. The efficiency shows no dependence on the structure (plate or tube) and the material (ceramic or glass) of the electrode.

As we mentioned above, κ was estimated to be 0.5 in former reports. Here we estimate it more exactly from our experimental results. The solid curve in figure 2 shows the efficiency assuming that $\kappa = 0.55$ in equation (7) for all E/N . As the experimental data points are in good agreement with this theoretical curve, the value of κ is estimated to be approximately 0.55. So, we assume $\kappa = 0.55$ for all discharge conditions in the theoretical analysis discussed in the following section.

Figure 2 shows that the maximum ozone yield decreases gradually with the increase of the reduced electric field strength when $E/N > 100$ Td. The operation at relatively low E/N of 80–120 Td is undoubtedly suitable for efficient generation of low-concentration ozone by a conventional ozone generator.

3. Theoretical investigation

3.1. Dissociation rate of ozone by electron impact

The electron energy dependence of the dissociation rate of ozone by electron impact has not been clarified yet. Therefore, it is assumed in the previous investigations that its reaction rate coefficient is constant, being independent of average electron energy (or electric field strength). The dissociation rate coefficient of ozone by electron impact k_6 , has been assumed to be in the form of $\alpha(k_1 + k_2)$, adjusting the result of analysis to the experimental result, where α is a constant, and k_1 and k_2 are the dissociation

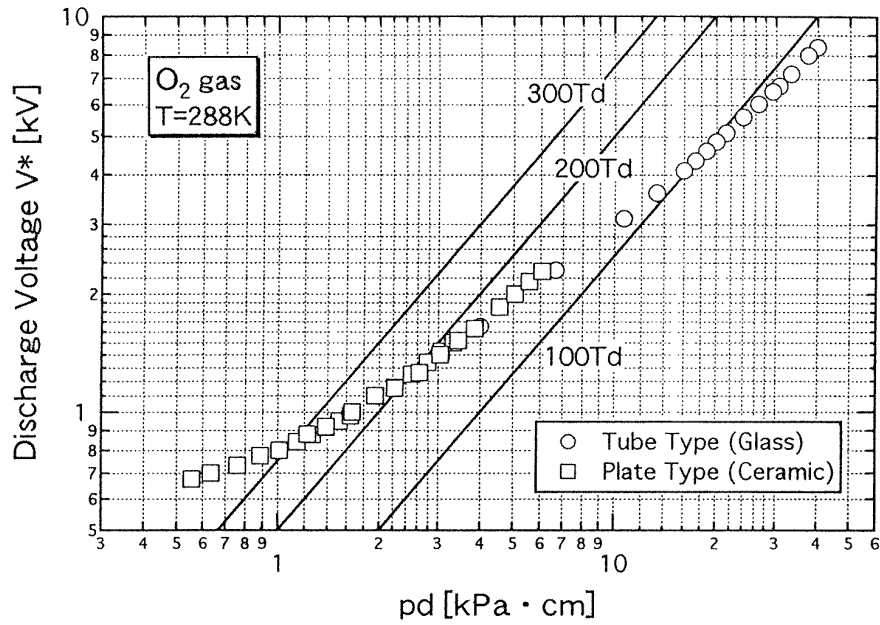


Figure 1. Measured discharge voltage as a function of pd .

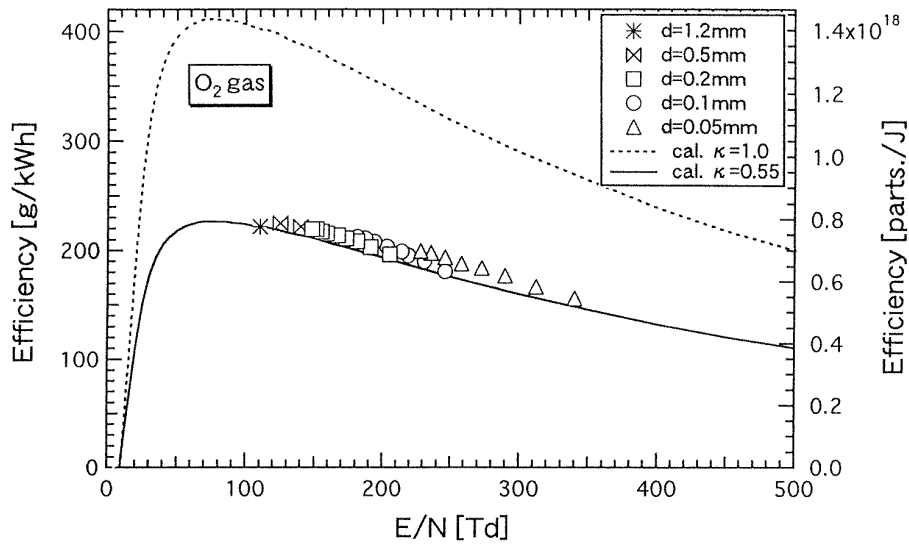


Figure 2. Maximum efficiency as a function of E/N .

rate coefficients of oxygen molecules in equations (2) and (3). But the reported values of α vary from 5 to about 30 [2, 3, 6, 7].

As far as the authors know, there is only one report on the dissociation cross section of ozone; we can refer only to the value calculated by Keto [8]. In this paper the dissociation rate coefficient of ozone in oxygen is obtained by using the cross section of the Keto report, assuming that the electron energy distribution does not change by the generation of ozone. Thus, the dissociation rate coefficient of ozone is given by

$$k_6 = \sqrt{\frac{2}{m}} \int \sqrt{\varepsilon} F_0(\varepsilon) Q(\varepsilon) d\varepsilon \quad (8)$$

where m is the mass of an electron, ε is the electron energy, $F_0(\varepsilon)$ is the energy distribution function of electron in oxygen, and $Q(\varepsilon)$ is the dissociation cross section of ozone.

The calculated ratio of the dissociation rate coefficient of ozone to that of oxygen, $\alpha = k_6/(k_1 + k_2)$, is shown by the dotted curve in figure 3. From figure 3, α decreases with increasing reduced electric field strength. Accordingly, the operation of an ozone generator with high electric field strength is clearly advantageous for producing high-concentration ozone by suppressing the decomposition of generated ozone.

In another report α was estimated from the difference between the dissociation energy of ozone and oxygen,

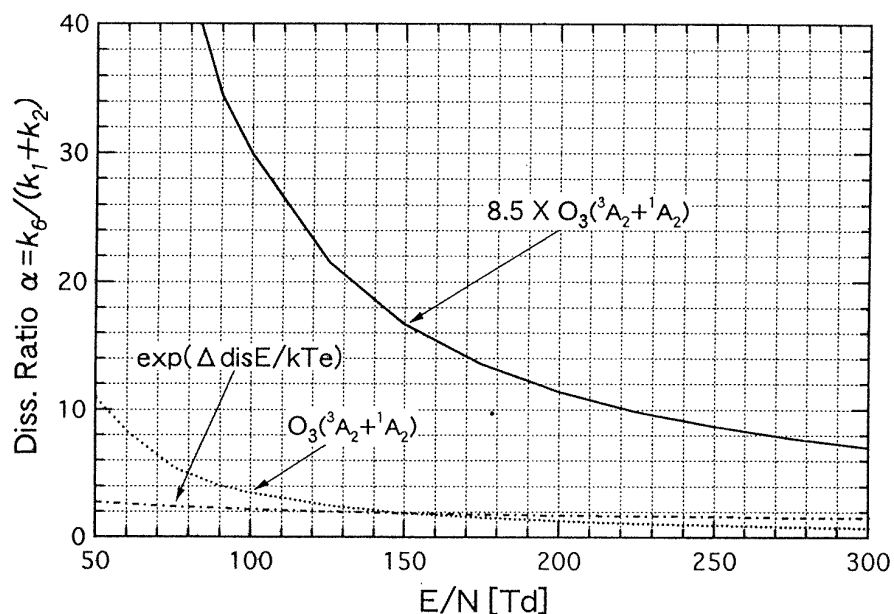


Figure 3. Estimated value for the ratio of the dissociation rate coefficient α .

expressing the decomposition rate coefficient of ozone as a function of electron energy [9]. They carried out the quantitative determination of ozone dissociation rate coefficient and gave α by

$$\alpha = \exp(\Delta_{dis}E/kT_e) = \exp(4/kT_e) \quad (9)$$

where $\Delta_{dis}E$ is the difference between the dissociation energy of ozone and oxygen, and kT_e is the electron energy. The calculated α values from equation (9) are also shown in figure 3 by the dot-dashed curve. It shows almost no dependence on the electron energy in contrast to the results calculated from equation (8). This analysis would lead to serious inaccuracy because of their assumptions such as Maxwellian electron energy distribution. Moreover, another assumption that the magnitude of the dissociation cross section for ozone is the same as that for oxygen is believed to be rather extreme.

Because the cross section for the dissociation of ozone reported by Keto is estimated on the basis of theoretical analysis, it is not guaranteed in the absolute value of its certainty. Moreover, there are some other dissociation levels which have similar profiles of cross sections to that reported by Keto, for example, $O_3(^1B_2)$ (threshold: 4.07 eV) and $O_3(^3B_2)$ (threshold: 2.92 eV). So, it is impossible to evaluate the actual dissociation rate of ozone by considering only the cross section reported by Keto. But the rate coefficients of these dissociation levels are expected to have a similar dependence on E/N as those shown in figure 3. Therefore, we can assume that the actual dissociation rate of ozone can be expressed as the product of a certain constant and the dissociation rate for $O_3(^3A_2+^1A_2)$ shown in figure 3. Considering the accordance of the theoretical results with the experimental results described in section 4, the estimation of the constant is estimated to be 8.5. Thus, the estimated dissociation rate

of ozone is given as a function of E/N shown in figure 3 by the solid curve. As described later, this estimation for the actual dissociation rate of ozone is shown to work fairly well in explaining the experimental ozone generation characteristics by our theoretical model. The solid curve in figure 3 shows the ratio of the dissociation rate coefficient of ozone to that of oxygen to be used in the analysis discussed later.

3.2. Gas temperature in discharge space

Since many of the rate coefficients used in our reaction scheme depend on temperature, we have to know the average gas temperature in the discharge gap. As we mentioned above, we assume a stationary and uniform discharge in time and space in this analysis. Therefore, the gas temperature dominating the ozone yield characteristics is assumed to be the time-averaged one in the discharge gap. Although the gas temperature varies along the direction of the discharge gap, we use the space-averaged temperature as the representative gas temperature in the discharge gap from the assumption.

Considering the balance between the power dissipated in the discharge gap and the heat removal by heat conduction to the cooled electrode, the average gas temperature T_{avg} is obtained by,

$$T_{avg} = \frac{1}{d} \int_0^d T(x) dx = \frac{W/S}{3k} d + T_{wall} \quad (10)$$

for an ozone generator with an externally cooled earth electrode, where x is the distance in the direction of the discharge gap, W is the discharge power, S is the discharge area (W/S is the areal discharge power density), d is the discharge gap length, k is the heat conductivity of oxygen ($2.674 \times 10^{-4} \text{ W cm}^{-1}\text{K}^{-1}$ at 300 K), and T_{wall}

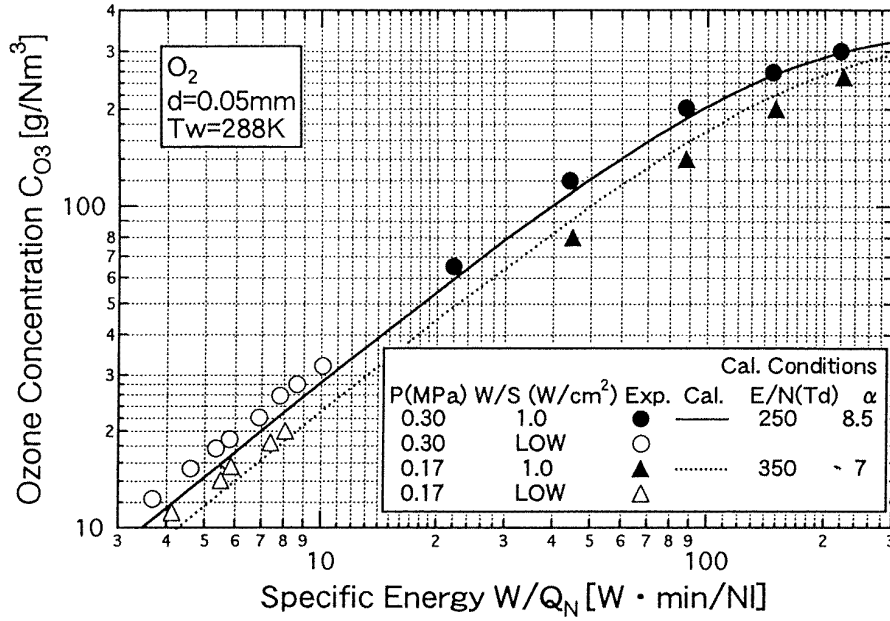


Figure 4. Experimental and calculation results for discharge gap length of 50 μm .

is the temperature of the surface of the cooled electrode. As the power portion used for ozone generation is small compared to the total discharge power, it is neglected in equation (10). Since the average temperature increase is not as large as 50 K under ordinary operating conditions, we can use the value of k at 300 K for all conditions, neglecting the dependence of heat conductivity on temperature. For an ozone generator with earth and high-voltage electrodes cooled externally, the average gas temperature is obtained by,

$$T_{avg} = \frac{1}{d} \int_0^d T(x) dx = \frac{W/S}{12k} d \left(\frac{4kt_g + k_g d}{k_g d + kt_g} \right) + T_{wall} \approx \frac{W/S}{12k} d + T_{wall} \quad (11)$$

where k_g and t_g are the heat conductivity and thickness of the glass or ceramic, respectively. Since k_g is much larger than k , we can assume $k_g d \gg kt_g$. Thus we obtain equation (11) in a simpler form.

3.3. Reaction scheme

In order to calculate ozone generation characteristics in silent discharge, we consider the reactions involving electrons, the ground states, $\text{O}(^3\text{P})$, $\text{O}_2(\text{X}^3\Sigma_g^-)$ and O_3 , and the several excited states, $\text{O}(^1\text{D})$, $\text{O}_2(\text{a}^1\Delta_g)$, $\text{O}_2(\text{b}^1\Sigma_g^+)$, $\text{O}_2(\text{A}^3\Sigma_u^+)$, $\text{O}_2(\text{B}^3\Sigma_u^-)$ and O_3^* , where O_3^* represents a vibrationally excited ozone molecule. In our reaction scheme, reactions involving ionic species are regarded to be of little importance in ozone generation and are neglected. Our reaction scheme considers 39 reactions listed in the appendix. We use the value for electron number density which is averaged in time and space in the same manner as the gas temperature mentioned above.

3.4. Assumptions for theoretical analysis

Here we summarize the assumptions in our ozone generation model: (1) discharge is stationary and uniform in time and space, (2) the portion of energy carried by electrons, κ , is 0.55, (3) the dissociation rate of ozone by electron impact is given in the form of the product of the constant, 8.5, and the dissociation rate for $\text{O}_3(^3\text{A}_2 + ^1\text{A}_2)$ as a function of the electric field strength (see figure 3), and (4) the time- and space-averaged gas temperature calculated from the homogeneous heat generation assumption ((10) or (11)) is used as the representative temperature.

4. Comparison with experimental results

The parameters that have the largest influence on ozone generation are the discharge gap length, gas pressure and gas temperature. The results of the theoretical calculations are compared with experimentally obtained results in the following subsections. All experimental and calculated results are summarized in the form of the relationship between ozone concentration C_{O_3} and specific energy W/Q_N , where Q_N is the flow rate of the source gas, namely, oxygen. W/Q_N represents the input discharge energy per molecule, and it is another important parameter that influences the ozone generation characteristics. The reduced electric field strength E/N is evaluated from the value of the discharge voltage V^* obtained from the $V-Q$ Lissajous figure, and it is thought to be the average electric field strength in the discharge gap.

4.1. Effect of electric field strength on ozone generation characteristics

Figure 4 shows the experimental and calculation results under the operating conditions of a discharge gap length

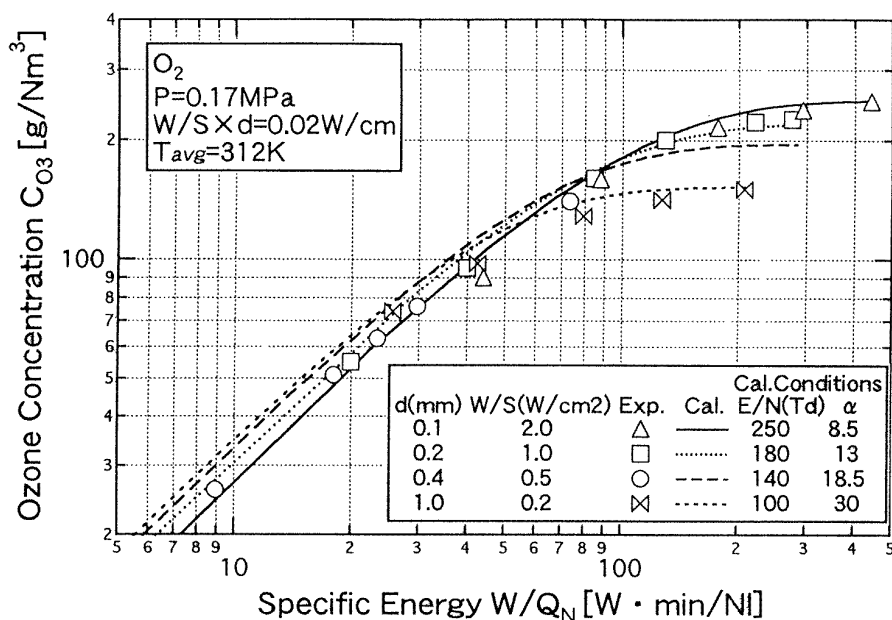


Figure 5. Ozone generation characteristics for various discharge gap lengths at constant gas pressure and temperature.

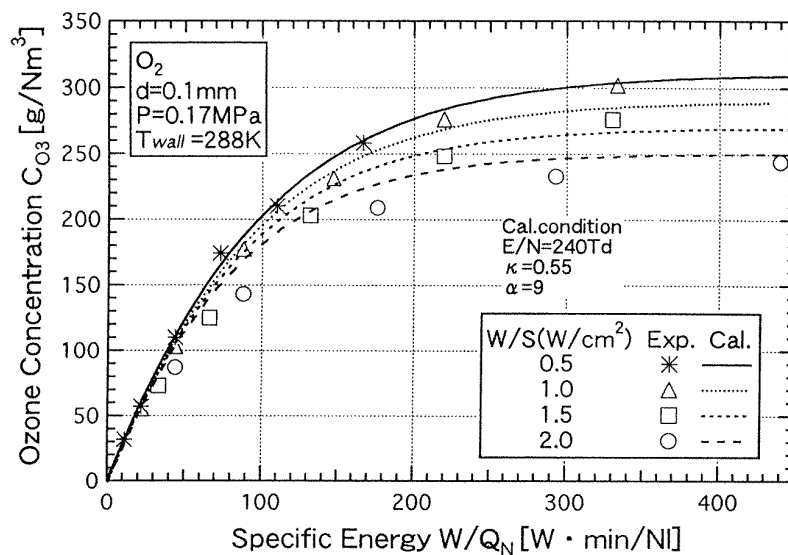


Figure 6. Dependence of ozone generation characteristics on discharge power density at $d = 0.1$ mm.

of $50 \mu\text{m}$ and a gas pressure of 1.7 and 3.0 atm. The calculation conditions used in this analysis are also indicated in the lower inset of figure 4. The unit, g/Nm^3 , on the vertical axis represents ozone concentration in standard conditions (273 K, 101.3 kPa). The experimental results are found to be in good accordance with the results of the calculations. The effect of gas pressure on the ozone generation characteristics for an oxygen-fed ozone generator with extremely short discharge gap length is summarized as follows: (1) over the region of low ozone concentration where all oxygen atoms dissociated by electron impact are transformed into ozone molecules by the three-body collision reaction, the efficiency of ozone

generation decreases with decreasing gas pressure because of the increase of the electric field strength E/N as shown in figure 2 in combination with figure 1, namely, the efficiency at a gas pressure of 1.7 atm is lower than that at a gas pressure of 3.0 atm, and (2) on the other hand, the effect of ozone dissociation by electron impact on ozone generation becomes small at low gas pressure (high E/N) as shown in figure 3. The efficiency at a gas pressure of 1.7 atm is not significantly different from that at 3.0 atm at high ozone concentrations, because the decreasing efficiency with pressure is compensated by a reduced destruction of ozone via electron collision processes.

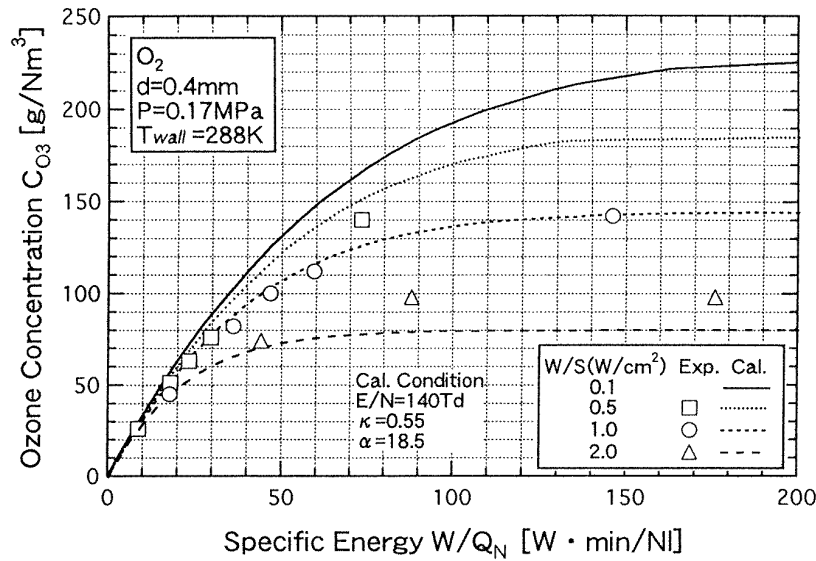


Figure 7. Dependence of ozone generation characteristics on discharge power density at $d = 0.4$ mm.

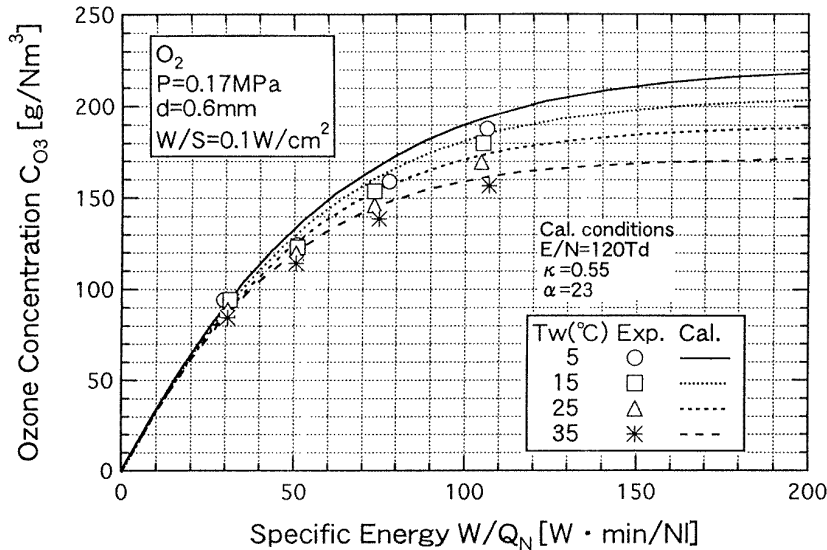


Figure 8. Dependence of ozone generation characteristics on cooling water temperature.

Figure 5 shows the results for several discharge gap lengths at a constant gas pressure of 1.7 atm. The calculation conditions used in the analysis are also indicated in the lower inset of figure 5. The experimental results are found to be in good accordance with the results of the calculations. Since the product of discharge power density W/S and discharge gap length d is constant for all conditions, the average gas temperature in the discharge space obtained from equation (10) is identical ($T_{avg} = 312$ K) throughout the four trials. The experimental and calculation results show that the maximum ozone concentration increases with decreasing discharge gap length. This is because the ozone dissociation by electron impact is likely to be suppressed by the high electric field strength E/N ; as shown in figure 3, the dissociation rate

ratio α decreases with the increase of the electric field strength E/N . Therefore, the production of significantly high-concentration ozone is shown to be possible by using an extremely short discharge gap and thus very high E/N operation.

4.2. Effect of gas temperature on ozone generation characteristics

The average gas temperature in the discharge space is the sum of two terms, the average gas temperature increase by discharge and the temperature of cooling water, as shown in equations (10) or (11). In this subsection we discuss the effect of these two terms on ozone yield characteristics from the results of experiment and calculation.

Figure 6 illustrates the dependence of ozone yield characteristics on discharge power density W/S at discharge gap length $d = 0.1$ mm and gas pressure $P = 1.7$ atm. Under these conditions the average gas temperature is estimated from (10) to be 294 K for $W/S = 0.5$ W cm⁻², 300 K for 0.1 W cm⁻², 306 K for 1.5 W cm⁻², and 313 K for 2.0 W cm⁻². The experimental and calculation results give fairly good accordance. While the ozone generation characteristics do not show any remarkable dependence on the discharge power density over the region of low specific energy (less than 50 W min/Nl), the attainable maximum ozone concentration and the efficiency of ozone generation decrease with increasing specific energy and discharge power density. Figure 7 shows similar results for the operation at $d = 0.4$ mm and $P = 1.7$ atm. Comparing these two figures, it is shown that the dependence of ozone yield characteristics on discharge power density is stronger for the operation at $d = 0.4$ mm than for that at $d = 0.1$ mm. Since the average gas temperature increase is proportional to the discharge gap length d (see equation (10) or (11)), the former operation gives four times higher gas temperature increase with identical increase of the power density than the latter one. It is no longer practical to operate with discharge power density $W/S = 1.0$ W cm⁻² or higher for discharge gap length $d = 0.4$ mm. The extremely short discharge gap length clearly gives another potential advantage to lower the gas temperature and thus to suppress the ozone decomposition.

Figure 8 shows the dependence of ozone generation characteristics on the temperature of cooling water for the operation at $d = 0.6$ mm and $P = 1.7$ atm. The experimental results are in fairly good accordance with the calculation results. Since a temperature increase of 10 K of cooling water causes an identical increase of gas temperature in the discharge space as shown in (10), the attainable maximum ozone concentration and the efficiency of ozone yield at high ozone concentration decrease simultaneously with the temperature increase of cooling water.

The reactions contributing to the decomposition of ozone are very sensitive to temperature and their rate coefficients become larger with temperature increase. It is impossible to efficiently generate high-concentration ozone at high gas temperatures because the decomposition of ozone is dominant. Accordingly, the efficient generation of high-concentration ozone requires us to lower the average gas temperature in the discharge space as much as possible. Because extremely short gap lengths for an oxygen-fed ozone generator are clearly concluded to show not only the advantage of forming high-strength electric field but also the advantage of suppressing gas temperature increase, their usage is a very effective means for the efficient generation of high-concentration ozone.

5. Conclusion

Ozone generation in silent discharges can be calculated from the reported electron collision cross sections and rate coefficients, considering the dependence of the dissociation

rate of ozone by electron impact on electric field strength in the discharge space. Our model consists of reactions for the dissociation of O₂ and O₃ by electron impact and reactions between oxygen species including the ground and excited states. By assuming the dissociation rate coefficient of ozone to be a function of electron energy, we have shown that our model can predict the performance of an oxygen-fed ozone generator very well for every operating condition examined. A more sophisticated model will give higher accuracy, and also more exact measurement of dissociation cross sections of ozone is desired to improve the accuracy of our simulation. It is concluded that the operation under high electric field has a strong advantage in generating high-concentration ozone efficiently because of the reduction in the population density of low-energy electrons which decompose generated ozone, i.e., the usage of extremely short gap lengths (around 100 μm) is one of the most advantageous means for the production of high-concentration ozone.

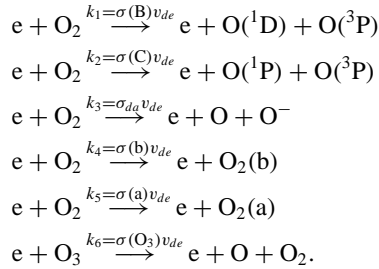
Acknowledgments

The authors wish to thank Dr N Tabata for his helpful discussion.

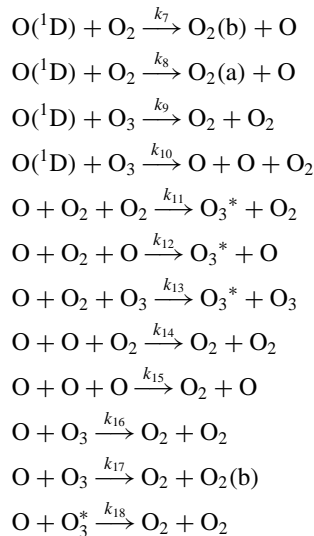
Appendix: list of reactions

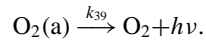
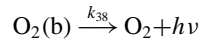
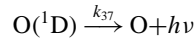
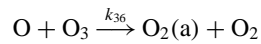
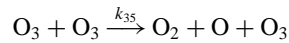
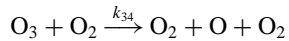
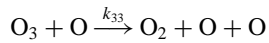
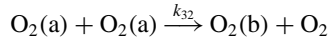
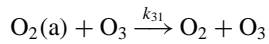
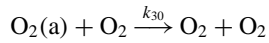
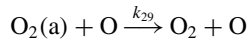
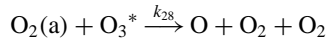
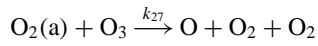
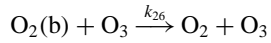
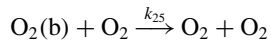
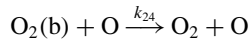
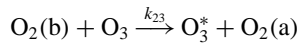
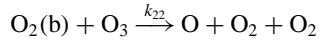
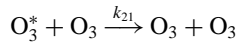
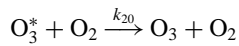
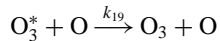
Reactions for ozone formation and decomposition considered in the analysis are shown below.

Reactions by electron impact



Reactions between oxygen species





References

- [1] Siemens W 1857 *Ann. Phys. Chem.* **102** 66–122
- [2] Yagi S and Tanaka M 1979 *J. Phys. D: Appl. Phys.* **12** 1509–20
- [3] Eliasson B, Hirth M and Kogelschatz U 1987 *J. Phys. D: Appl. Phys.* **20** 1421–37
- [4] Kuzumoto M, Tabata Y, Yoshizawa K and Yagi S 1996 *Trans. IEE Japan A* **116** 121–7
- [5] Tabata N, Tanaka M and Yagi S 1977 *Trans. IEE Japan B* **97** 100
- [6] Samoilovich V G, Popovich M P, Emel'yanov Y M and Filippov Y V 1966 *Russ. J. Phys. Chem.* **40** 287–90
- [7] Devins J C 1956 *J. Electrochem. Soc.* **103** 460–6
- [8] Keto J W 1981 *J. Chem. Phys.* **74** 4445–9
- [9] Sadadil H, Bachmann P and Kastelewicz G 1984 *Beitr. Plasma Phys.* **81** 423–4